An Improved Arbitrary-Radius-Wire Representation for FDTD Electromagnetic and Surge Calculations

Y. Taniguchi, Y. Baba, N. Nagaoka, A. Ametani

Abstract--In this paper, it is shown that finite-difference time-domain (FDTD) electromagnetic computations for a conductor system having a radius smaller than $0.15\Delta r$ or larger than $0.65\Delta r$ (Δr is the lateral side length of cells employed), which is modeled using arbitrary-radius-wire representations proposed so far with a time increment determined from the upper limit of Courant's stability condition, result in numerical instability. A primary factor causing this numerical instability is that the speed of waves propagating in the radial direction from the wire in the immediate vicinity of the wire exceeds the speed of light, and therefore, Courant's condition is not satisfied there. Further, it is shown that the arbitrary-radius-wire representation can be improved by modifying the material parameters as follows. In representing a wire whose radius is smaller than the equivalent radius ($a_0 = 0.230\Delta r$ or $0.208\Delta r$) using the improved technique, the permeability for calculating the axial magnetic field components closest to the wire and for calculating the circulating magnetic field components closest to and half cell away from the tip of the wire is modified in addition to the permeability and the permittivity for calculating the circulating magnetic field components and the radial electric field components, closest to the wire, respectively. In representing a wire whose radius is larger than a_0 using the technique, the permittivity for calculating the axial electric field components closest to the wire is modified in addition to the permittivity and the permeability for calculating the radial electric field components and the circulating magnetic field components, respectively. The improved wire representation is effective in representing a wire whose radius ranges from $0.0001\Delta r$ to $0.9\Delta r$.

Keywords: electromagnetic fields, finite difference time domain methods, transient analysis, wire.

I. INTRODUCTION

THE finite-difference time-domain (FDTD) method for solving Maxwell's equations [1][2] has been widely used in analyzing transient electromagnetic fields. In FDTD computations, it would be quite useful if a wire having an arbitrary radius could be simply and accurately represented regardless of the size of cells employed. Umashankar et al. [3], Noda and Yokoyama [4], and Railton et al. [5][6] have proposed arbitrary-radius-wire representations for FDTD

computations in the three-dimensional (3D) Cartesian coordinate system. Note that Holland and Simpson [7], and Makinen et al. [8] have also proposed arbitrary-radius-wire representations, and Edelvik [9] has proposed an arbitrarily-oriented-thin-wire representation. Also note that Taniguchi et al. [10] have proposed an arbitrary-radius-wire representation in the 2D cylindrical coordinate system.

Umashankar et al. have shown that a perfectly conducting wire, represented by forcing the tangential components of electric field along the wire axis to zero in FDTD computations in the 3D Cartesian coordinate system, has an equivalent radius, $a_0 = 0.135\Delta r$, where Δr is the lateral side length of cells used. Noda and Yokoyama, and Railton et al. have shown that a perfectly conducting wire represented in the same manner as done by Umashankar et al. has an equivalent radius, $a_0 = 0.230\Delta r$ and $0.208\Delta r$, respectively. Further, Umashankar et al. have represented a wire having an arbitrary radius, a, by changing the integral length of radial electric field from Δr to ($\Delta r - a$) in calculating the circulating magnetic field components closest to the wire. Noda and Yokoyama, and Railton et al. have represented an arbitrary-radius wire by embedding the wire of $a_0 = 0.230\Delta r$ and $0.208\Delta r$, respectively, in a relevant artificial parallelepiped medium. In order to represent a thinner wire in air than the wire having the corresponding equivalent radius, a_0, the relative permeability for calculating the circulating magnetic field components closest to the wire needs to be increased and the relative permittivity for calculating the closest radial electric field components needs to be reduced. Note that the wire representations proposed by Noda and Yokoyama, and Railton et al. are more effective than that proposed by Umashankar et al.

However, FDTD computations for a conductor system having a radius, a, smaller than $0.15\Delta r$ or larger than $0.65\Delta r$, modeled using the wire representations of Noda and Yokoyama, and Railton et al., with a time increment determined from the upper limit of Courant stability condition (about $0.99\Delta r/c/\sqrt{3}$, where c is the speed of light), result in numerical instability (this will be shown in Section II. B in this paper). This indicates that the smallest radius of a wire, which can be modeled appropriately using these wire representations, would be 0.15 m if cubic cells whose side length is $\Delta r = 1$ m is employed. This radius, 0.15 m, is not sufficiently small for representing actual overhead telecommunication, power transmission, and distribution wires. Although it is shown that FDTD computations can be carried out stably for a conductor system whose radius is

smaller than $0.1\Delta r$ if a smaller time increment such as $0.7\Delta r/c/\sqrt{3}$ or $0.8\Delta r/c/\sqrt{3}$ [6][11] is employed, this increases the computation time and would increase the error due to grid dispersion.

In this paper, an improved representation of an arbitrary-radius wire, which enables FDTD computations in the 3D Cartesian coordinates to be carried out stably and accurately with a time step determined from the upper limit of Courant's stability condition, follows. In Section II, the arbitrary-radius-wire representations proposed by Noda and Yokohama, and Railton et al. are reviewed and the range within which FDTD computations can be carried out stably is indicated. In Section III, the causes for the numerical instability that occurs in FDTD computations using these thin wire representations are exposed and an improved wire representation is presented. In Section IV, the validity of the improved wire representation is demonstrated.

II. ARBITRARY-RADIUS-WIRE REPRESENTATIONS PROPOSED SO FAR AND THEIR NUMERICAL INSTABILITY

A. Arbitrary-Radius-Wire Representations Proposed So Far

In this section, we briefly review representations proposed by Noda and Yokoyama [4], and Railton et al. [5].

Noda and Yokoyama represent a wire having an arbitrary radius, a, by embedding a wire having an equivalent radius, $a_0 = 0.230\Delta r$, in an artificial parallelepiped medium. The relative permeability, μ_r', for calculating the circulating magnetic field components closest to the wire and the relative permittivity, ε_r', for calculating the closest radial electric field components are given by

$$\mu_r' = \mu_r / m, \qquad \varepsilon_r' = m\varepsilon_r,$$
$$m = \frac{\ln(\Delta r / a_0)}{\ln(\Delta r / a)}, \qquad a_0 = 0.230\Delta r, \qquad (1)$$

where μ_r and ε_r are the relative permeability and permittivity of the original medium surrounding the wire, a_0 is the equivalent radius (represented by forcing the tangential components of electric field along the wire axis to zero).

Railton et al. represent a wire having an arbitrary radius similarly. The material parameters that should be employed are given by

$$\mu_r' = \mu_r / m, \qquad \varepsilon_r' = m\varepsilon_r,$$
$$m = \frac{2\tan^{-1}\left(\Delta r / \Delta r\right)}{\ln\left(\Delta r / a\right)}\frac{\Delta r}{\Delta r} = \frac{\pi / 2}{\ln\left(\Delta r / a\right)} \qquad (2)$$

The equivalent radius of a wire, represented simply by forcing the tangential components of electric field along the wire to zero, is given from (2) by $a_0 = 0.208\Delta r$ [$=\Delta r/\exp(\pi/2)$].

Note that, in the above two representations, the speed of an electromagnetic wave propagating in the axial direction in the immediate vicinity of the wire is equal to the speed of light, c (or it is not changed by this modification) since $m\varepsilon_r\varepsilon_0\mu_r\mu_0/m = \varepsilon_r\varepsilon_0\mu_r\mu_0$.

B. Numerical Instability

In this section, we show that the radius range within which FDTD computations can be carried out stably and accurately with a time increment determined from the upper limit of Courant's stability condition.

Fig. 1 shows a conductor system to be used for this aim. A 4 m long horizontal wire is located 0.5 m above perfectly conducting ground. The horizontal conductor is excited at one of its ends by a lumped voltage source located on perfectly conducting ground via a vertical current lead wire. The other end of the horizontal conductor is open. The lumped voltage source generates a ramp wave having a magnitude of 100 V and a risetime of 5 ns. The working volume of 6 m × 6 m × 6m is divided into cubic cells whose side length is Δr=50 mm, and is surrounded by five planes of Liao's second-order absorbing boundary [12] other than the bottom perfectly conducting plane. The time increment is set to 0.99 of the upper limit of Courant's stability condition ($0.99\Delta r/c/\sqrt{3}$).

We compare the characteristic impedance values, evaluated as the ratio in magnitudes of the applied voltage and the conductor current in a quasi-steady state, with the corresponding theoretical values given by

$$Z_c = 60\ln(2h/a) \qquad (3)$$

where h is the height of a horizontal wire, and a is its radius. Table I shows FDTD-calculated characteristic impedance values with the arbitrary-radius-representations for a wire radius ranging from a=2.5 mm (=$0.05\Delta r$) to 35 mm (=$0.7\Delta r$), and the corresponding theoretical values calculated using (3). When $a < 0.15\Delta r$ or $a > 0.65\Delta r$, the FDTD computation suffers from numerical instability. When $0.15\Delta r \leq a \leq 0.65\Delta r$, the FDTD computation is carried out stably and accurately (the differences between the FDTD-calculated values and the corresponding theoretical values are less than about 1%).
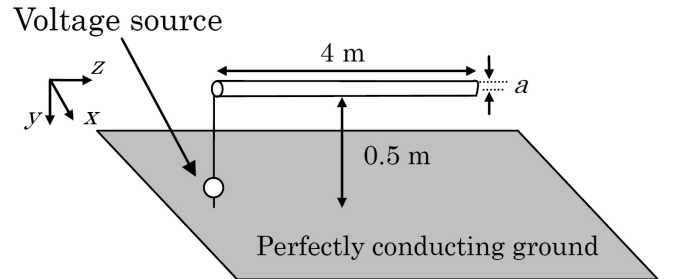
Fig. 1.   An open-ended horizontal wire of length 4 m excited by a lumped voltage source.

TABLE 1.   RANGE IN WHICH FDTD COMPUTATIONS CAN BE CARRIED OUT STABLY WITH ARBITRARY-RADIUS-WIRE REPRESENTATIONS PROPOSED BY NODA AND YOKOYAMA, AND RAILTON ET AL.

	Wire radius, a		
	From $0.05\Delta r$ to $0.1\Delta r$	From $0.15\Delta r$ to $0.65\Delta r$	$0.7\Delta r$
Noda and Yokoyama	unstable	stable (1%)	unstable
Railton	unstable	stable (1%)	unstable

Note that, although it is known that the use of a time increment, $0.7\Delta r/c/\sqrt 3$ or $0.8\Delta r/c/\sqrt 3$ [6][11] makes it possible to carry out an FDTD computation stably for a thinner wire than $0.1\Delta r$, the reason has not been clarified. Also, it increases the computation time and would increase the error due to the grid dispersion. Therefore, the use of smaller time increment is not a good countermeasure to the numerical instability. In the following section, we will propose an improved wire representation, which will make it possible to carry out an FDTD computation stably and accurately even when the wire radius is out of the range from $0.15\Delta r$ to $0.65\Delta r$.

III.   AN IMPROVED ARBITRARY-RADIUS-WIRE REPRESENTATION

A. A Factor Causing Numerical Instability

In this section, we investigate the cause of numerical instability when an FDTD computation is carried out for a conductor system having a radius smaller than $0.15\Delta r$ or larger than $0.65\Delta r$, modeled using the wire representations proposed by Noda and Yokoyama [4], and Railton et al. [5], with a time increment determined from the upper limit of Courant's stability condition ($0.99\Delta r/c/\sqrt 3$).

Fig. 2 shows the relations between the modified coefficient, m, and the wire radius, a. In the representation of Noda and Yokoyama, $m=1$ when $a=a_0=0.230\Delta r$. In the representation of Railton et al., $m=1$ when $a=a_0=0.208\Delta r$. In either representation, $m < 1$ when $a < a_0$, and $m > 1$ when $a > a_0$.

Equation (4) shows update equations for the radial electric field components, E_x and E_y, and the axial electric field component, E_z, closest to a z-directed wire. Equation (5) shows update equations for the closest circulating magnetic field components, H_x and H_y, and the closest axial magnetic field component, H_z. In representing a wire whose radius a is smaller than a_0, the modification coefficient, m, is smaller than 1. Since the permittivity for calculating E_x and E_y [see (4a) and (4b)] is $m\varepsilon_r\varepsilon_0$ and the permeability for calculating H_x and H_y [see (5a) and (5b)] is $\mu_r\mu_0/m$, the propagation speed of electromagnetic waves in the direction of the poynting vectors of E_x and H_y, and E_y and H_x, which is the z-direction, is equal to the speed of light [$(m\varepsilon_r\varepsilon_0\mu_r\mu_0/m)^{-1/2}=(\varepsilon_r\varepsilon_0\mu_r\mu_0)^{-1/2}$]. However, since the permeability for calculating H_z is $\mu_r\mu_0$ [see (5c)], the propagation speed of an electromagnetic wave in the direction

of the poynting vector of E_x and H_z, and E_y and H_z, which are the y- and x-directions, respectively, exceeds the speed of light [$(m\varepsilon_r\varepsilon_0\mu_r\mu_0)^{-1/2}=c/\sqrt m > c$ for $m < 1$]. The time increment determined from the upper limit of Courant's stability condition ($0.99\Delta r/c/\sqrt 3$), with an assumption of the wave propagation speed being equal to c, does not satisfy Courant's stability condition for electromagnetic waves whose propagation speed is greater than c. This is probably a primary factor that causes numerical instability, and also a reason why the numerical instability is avoided when a smaller time increment is employed.

$$E_x{}^n = E_x{}^{n-1} + \frac{\Delta t}{m\varepsilon_r\varepsilon_0}\left(\frac{\partial H_z^{n-1/2}}{\partial y} - \frac{\partial H_y^{n-1/2}}{\partial z}\right), \qquad (4a)$$

$$E_y{}^n = E_y{}^{n-1} + \frac{\Delta t}{m\varepsilon_r\varepsilon_0}\left(\frac{\partial H_x^{n-1/2}}{\partial z} - \frac{\partial H_z^{n-1/2}}{\partial x}\right), \qquad (4b)$$

$$E_z{}^n = E_z{}^{n-1} + \frac{\Delta t}{\varepsilon_r\varepsilon_0}\left(\frac{\partial H_y^{n-1/2}}{\partial x} - \frac{\partial H_x^{n-1/2}}{\partial y}\right), \qquad (4c)$$

$$H_x{}^{n+1/2} = H_x{}^{n-1/2} - \frac{\Delta t}{\mu_r\mu_0/m}\left(\frac{\partial E_z^{n}}{\partial y} - \frac{\partial E_y^{n}}{\partial z}\right), \qquad (5a)$$

$$H_y{}^{n+1/2} = H_y{}^{n-1/2} - \frac{\Delta t}{\mu_r\mu_0/m}\left(\frac{\partial E_x^{n}}{\partial z} - \frac{\partial E_z^{n}}{\partial x}\right), \qquad (5b)$$

$$H_z{}^{n+1/2} = H_z{}^{n-1/2} - \frac{\Delta t}{\mu_r\mu_0}\left(\frac{\partial E_y^{n}}{\partial x} - \frac{\partial E_x^{n}}{\partial y}\right), \qquad (5c)$$

In representing a wire whose radius, a, is larger than a_0, the modification coefficient, m, is larger than 1. The propagation speed of electromagnetic waves in the direction of the poynting vectors of E_y and H_x, and E_x and H_y, which is the z-direction, is equal to the speed of light [$(m\varepsilon_r\varepsilon_0\mu_r\mu_0/m)^{-1/2} =(\varepsilon_r\varepsilon_0\mu_r\mu_0)^{-1/2}=c$]. On the other hand, the propagation speed of an electromagnetic wave in the direction of the poynting vector of E_z and H_x, and E_z and H_y, which are the y- and x-directions, respectively, exceeds c [$(\varepsilon_r\varepsilon_0\mu_r\mu_0/m)^{-1/2}=\sqrt m \times c > c$ for $m > 1$]. This causes numerical instability.
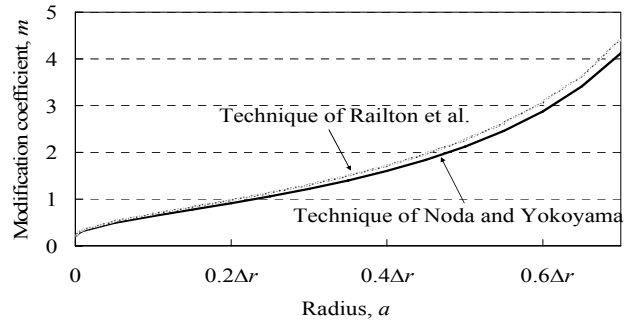
Fig. 2.   Relation between the modification coefficient, m, and the wire radius, a.

B. An Improved Wire Representation

In this section, in order to avoid the numerical instability, caused by the wave propagation speed greater than c in the radial direction in the immediate vicinity of a wire, we propose an improved wire representation. In the improved representation, we modify the permeability for calculating the axial magnetic field components closest to a wire or the permittivity for calculating the closest axial electric field components, depending on the wire radius ($a < a_0$ or $a > a_0$), in addition to the conventional modification for the closest circulating magnetic and radial electric field components.

In representing a z-directed wire whose radius, a, is smaller than the equivalent radius, a_0, the modified relative permeability, μ_r', given by (1) or (2), should be employed in calculating the axial magnetic field components closest to a wire, H_z [see Fig. 3 (a)], in addition to the closest circulating magnetic field components, H_x and H_y. This modification makes the wave propagation speed in the direction of the poynting vector of E_x and H_z (y-direction) and E_y and H_z (x-direction) in the immediate vicinity of the wire be equal to c since $(m\varepsilon_r\varepsilon_0\mu_r\mu_0/m)^{-1/2}=(\varepsilon_r\varepsilon_0\mu_r\mu_0)^{-1/2}$.

In representing a z-directed wire whose radius, a, is larger than a_0, the modified relative permittivity, ε_r', given by (1) or (2), should be employed in calculating the axial electric field components closest to a wire, E_z [see Fig. 3 (b)], in addition to the closest radial electric field components, E_x and E_y. This modification makes the wave propagation speed in the direction of the poynting vector of E_z and H_x (y-direction) and E_z and H_y (x-direction) in the immediate vicinity of the wire be equal to c. Note that, in representing a z-directed wire of $a > a_0$ located in a lossy medium whose conductivity is σ, one has only to employ $\sigma'=m\sigma$ [13] as well as $\varepsilon_r'=m\varepsilon_r$ in calculating the closest axial electric field components, E_z, in addition to the closest radial electric field components, E_x and E_y.

Note that, in representing a wire whose radius a is smaller than a_0 ($m < 1$), the relative permeability in calculating circulating magnetic field components closest to and half cell away from the tip of the wire should be modified. Although the permittivity for calculating the radial electric field components, E_x and E_y, at the tip ($z=k\Delta z$) of a z-directed wire shown in Fig. 4 is $m\varepsilon_r\varepsilon_0$, the permeability for calculating the circulating magnetic field components, H_x and H_y, at $z=(k+1/2)\Delta z$ is $\mu_r\mu_0$. Therefore, the propagation speed of electromagnetic waves in the direction of the poynting vectors of E_x and H_y, and E_y and H_x, which is the z-direction, exceeds the speed of light $[(m\varepsilon_r\varepsilon_0\mu_r\mu_0)^{-1/2}=(m\varepsilon_r\varepsilon_0\mu_r\mu_0)^{-1/2}=c/\sqrt{m} > c$ for $m < 1]$. This causes numerical instability. In order to avoid the numerical instability, the permeability for calculating H_x and H_y at $z=(k+1/2)\Delta z$ needs to be set to $\mu_r\mu_0/m$. In representing a wire whose radius a is larger than a_0 ($m > 1$), the propagation speed of electromagnetic waves in the direction of the poynting vectors of E_x and H_y, and E_y and H_x, which is the z-direction, is lower than the speed of light $[(m\varepsilon_r\varepsilon_0\mu_r\mu_0)^{-1/2}=(m\varepsilon_r\varepsilon_0\mu_r\mu_0)^{-1/2}=c/\sqrt{m} < c$ for $m > 1]$. This does not cause numerical instability.

We expect that FDTD computations will be carried out stably by employing, $\mu_r'=\mu_r/m$, in calculations of H_z closest to the wire and H_x and H_y closest to and half cell away from the tip of the wire for the case of $a < a_0$, and $\varepsilon_r'=m\varepsilon_r$ (and $\sigma'=m\sigma$), in calculation of E_z closest to the wire for the case of $a > a_0$.

(a) $a < a_0$ ($m < 1$)

(b) $a > a_0$ ($m > 1$)
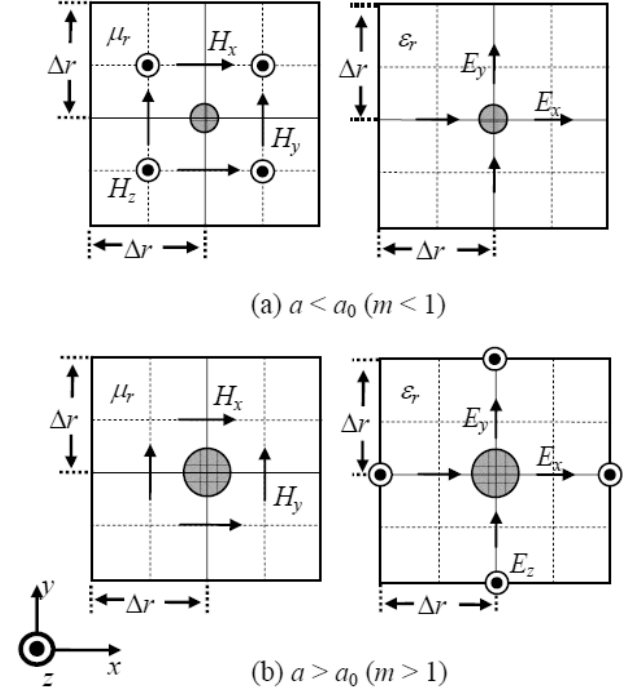
Fig. 3. A z-directed thin wire and the configuration of electric and magnetic field components closest to the wire.
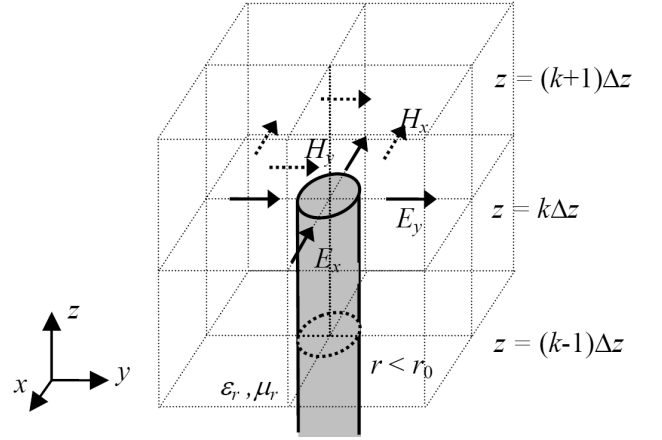
Fig. 4. Electric and magnetic field components closest to the tip of a z-directed wire.

IV. TESTING THE VALIDITY OF THE IMPROVED WIRE REPRESENTATION

In this section, we test the validity of the improved wire representation proposed in Section III. B.

An FDTD computation is carried out for the 4 m long perfectly conducting horizontal wire located 0.5 m above perfectly conducting ground, which is shown in Fig. 2. The working volume of 6 m × 6 m × 6 m is divided into cubic cells

whose side length is Δr=125 mm. Therefore, the equivalent radius of the horizontal wire is a_0=28.75 mm (=0.230Δr or 0.208Δr). The horizontal wire whose radius ranges from a=0.0125 mm (=0.0001Δr) to 112.5 mm (=0.9Δr), is represented using the improved wire representation. The time increment is set to 0.99$\Delta r/c/\sqrt{3}$.

Fig. 5 shows FDTD-calculated characteristic impedance values for the horizontal wire with the improved wire representation and the corresponding theoretical values calculated using (3). The FDTD computations are carried out stably for the whole range from a=0.0125 mm (=0.0001Δr) to 112.5 mm (=0.9Δr). Also, the FDTD-calculated values agree well with the corresponding theoretical values. The maximum difference is about 5%.

Fig. 6 shows waveforms of voltage and current measured by Noda and Yokoyama [4] for a horizontal wire whose configuration is similar to that shown in Fig. 1, and the corresponding waveforms calculated using the FDTD method with the improved wire representation. The ground conductivity is set to 5.9×10^7 S/m in order to simulate the copper plate used in the experiment. The length of the horizontal wire is 4 m, and the radius is 15 mm. The radius of a vertical lead wire, which connects a lumped voltage source having 50 Ω internal impedance with one end of the horizontal wire, is 10 mm. Since cubic cells whose side length is Δr=125 mm are used in the FDTD computation, the equivalent radius is a_0=0.230Δr=28.75 mm. The radii of the horizontal and vertical wires, a=15 mm (=0.12Δr) and 10 mm (=0.088Δr), are smaller than the equivalent radius, a_0=0.230Δr. Therefore, in representing these wires, the modified relative permeability, $\mu_r'=\mu_r/m$, is used for calculating the closest axial magnetic field components in addition to the closest circulating magnetic field components. The time increment is set to 0.99$\Delta r/c/\sqrt{3}$. The FDTD-calculated waveforms agree well with the corresponding measured waveforms.

The above results show that a wire whose radius ranges from 0.0001Δr to 0.9Δr can be modeled appropriately using the improved wire representation, while the conventional representations reduce the range of possible radii from 0.15Δr to 0.65Δr.
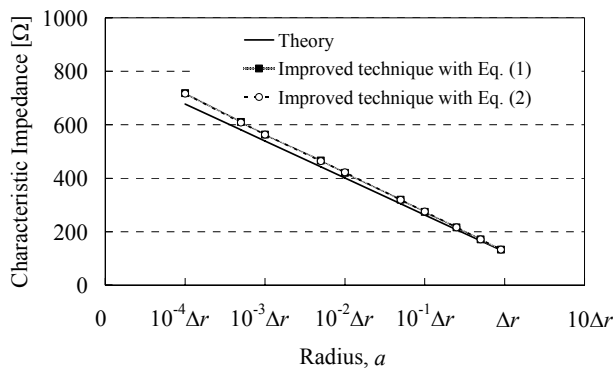
Fig. 5. FDTD-calculated and measured characteristic impedance values for a horizontal conductor.
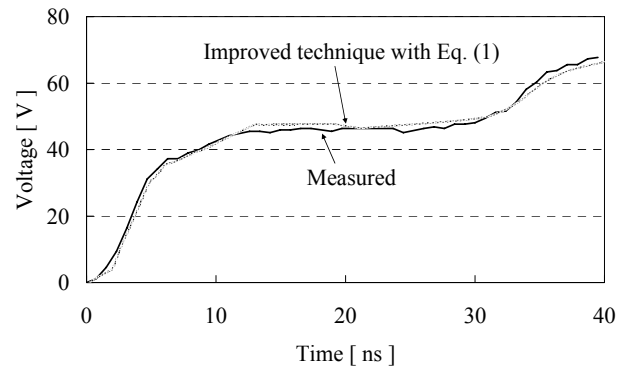
(a) Voltage
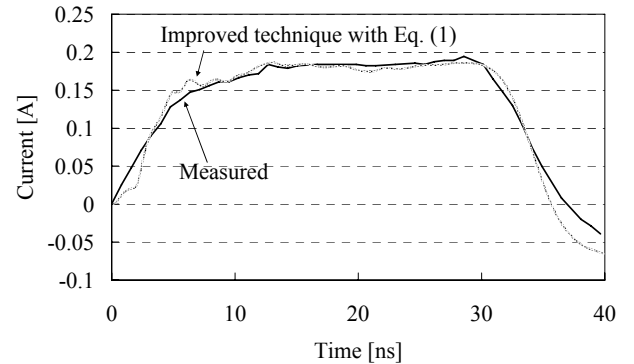
(b) Current

Fig. 6. FDTD-calculated and measured [4] waveforms of voltage and current for a horizontal conductor.

V. CONCLUSIONS

In FDTD computations, a wire represented by forcing the tangential components of electric field along the wire axis to zero has an equivalent radius, a_0=0.230Δr or 0.208Δr, where Δr is the lateral side length of cells employed. Arbitrary-radius-wire representations proposed by Noda and Yokoyama, Railton et al., in which an arbitrary-radius wire is represented by embedding the wire of equivalent radius, a_0, in an artificial parallelepiped medium, have been used. In this paper, it is shown that FDTD computations for a conductor system having a radius smaller than 0.15Δr or larger than 0.65Δr, modeled using these representations with a time increment determined from the upper limit of Courant's stability condition (0.99$\Delta r/c/\sqrt{3}$, where c is the speed of light), result in numerical instability. A primary factor causing this numerical instability is that the speed of waves propagating outward in the radial direction from the wire in the immediate vicinity of the wire exceeds c, and therefore, Courant's condition is not satisfied there. Further, it is shown that the arbitrary-radius-wire representation can be improved by modifying the material parameters as follows. In representing a wire whose radius is smaller than the equivalent radius a_0 using the improved technique, the permeability for calculating the axial magnetic field components closest to the wire and for calculating the circulating magnetic field components closest

to and half cell away from the tip of the wire is modified in addition to the permeability and the permittivity for calculating the circulating magnetic field components and the radial electric field components, closest to the wire, respectively. In representing a wire whose radius is larger than a_0 using the technique, the permittivity for calculating the axial electric field components closest to the wire is modified in addition to the permittivity and the permeability for calculating the radial electric field components and the circulating magnetic field components, respectively. The improved wire representation is effective in representing a wire whose radius ranges from $0.0001\Delta r$ to $0.9\Delta r$.

VI. REFERENCES

[1] K. S. Yee, "Numerical solution of initial boundary value problems involving Maxwell's equations in isotropic media," *IEEE Trans. Antennas Propag.*, vol. 14. no. 3, pp. 302-307, May 1966.

[2] A. Taflov, and S. C. Hagness, Computational Electromagnetics: The Finite-Difference Time-Domain Method, Norwood, M.A.: Artech House, Jun. 2000.

[3] K. R. Umashankar, A. Taflov, and B. Beker, "Calculation and experimental validation of induced currents on coupled wires in an arbitrary shaped cavity," *IEEE Trans. Antennas Propag.,* vol. 35, no. 11, pp. 1248-1257, Nov. 1987.

[4] T. Noda, and S. Yokoyama, "Thin wire representation in finite difference time domain surge simulation," *IEEE Trans. Pow. Deliv.*, vol. 17, no. 3, pp. 840-847, Jul. 2002.

[5] C. J. Railton, D. F. Paul, I. J. Craddock, and G. S. Hilton, "The treatment of geometrically small structures in FDTD by the modification of assigned material parameters," *IEEE Trans. Antennas Propag.*, vol. 53, no. 12, pp. 4129-4136, Dec. 2005.

[6] C. J. Railton, D. L. Paul, and S. Dumanli, "The treatment of thin wire and coaxial structures in lossless and lossy media in FDTD by the modification of assigned material parameters," *IEEE Trans. Electromagn. Compat.*, vol. 48, no. 4, pp. 654-660, Nov. 2006.

[7] R. Holland and L. Simpson, "Finite-difference analysis of EMP coupling to thin struts and wires," *IEEE Trans. Electromagn. Compat.*, vol. 23, no. 2, pp.88-97, May 1981.

[8] R. M. Makinen, J. S. Juntunen, and M. A. Kivikoski, "An improved thin-wire model for FDTD," *IEEE Trans. Microwave Theory and Techniques*, vol. 50, no. 5, pp.1245-1255, May 2002.

[9] F. Edelvik, "A new technique for accurate and stable modeling of arbitrary oriented thin wires in the FDTD method," *IEEE Trans. Electromagn. Compat.*, vol. 45, no. 2, pp.88-97, May 2003.

[10] Y. Taniguchi, Y. Baba, N. Nagaoka, and A. Ametani, "Representation of an arbitrary-radius wire for FDTD calculations in the 2D cylindrical coordinate system," *IEEE Trans. Electromagn. Compat.*, vol. 50, no. 4, pp. 1014-1018, Nov. 2008.

[11] E. T. Tuma, R. Oliveira, and C. L. da S. S. Sobrinho, "New model of current impulse injection and potential measurement in transient analysis of grounding systems in homogeneous and stratified soils using the FDTD method," *Proc. VIII Int. Symp. Lightning Protection*, pp. 526-531, Sao Paulo, Brazil, Nov. 2005.

[12] Z. P. Liao, H. L. Wong, B. –P. Yang, and Y. –F. Yuan, "A transmitting boundary for transient wave analysis," *Science Sinica,* vol.A27, no.10, pp.1063-1076. 1984.

[13] Y. Baba, N. Nagaoka, and A. Ametani, "Modeling of thin wires in a lossy medium for FDTD simulations," *IEEE Trans. Electromagn. Compat.*, vol. 47, no. 1, pp. 54-60, Feb. 2005.